

All-optical beam deflection and switching in strontium–barium–niobate waveguides

D. Kip,^{a)} M. Wesner, and E. Krätzig

Fachbereich Physik, Universität Osnabrück, 49069 Osnabrück, Germany

V. Shandarov

State University of Control Systems and Radioelectronics, Tomsk 634050, Russia

P. Moretti

Laboratoire de Physico–Chimie des Matériaux Luminescents, Université Claude Bernard, Lyon 1, 69622 Villeurbanne, France

(Received 19 November 1997; accepted for publication 23 February 1998)

Self-focusing by thermal heating because of absorption of a guided light beam in a planar strontium–barium–niobate waveguide is of interest for all-optical data processing. When a guided probe beam intersects the pump beam under a small angle inside the waveguide, the self-focusing effect in conjunction with self-bending because of the photorefractive effect can be used for large angle deflection of the probe beam and for switching with time constants of fractions of milliseconds. Deflection angles of the outcoupled probe light up to 0.23 rad in air and frequencies up to 3 kHz for optical switching are reached in the experiment. © 1998 American Institute of Physics. [S0003-6951(98)02616-3]

Recently considerable attention has been focused on the development of components for all-optical data processing, like beam deflectors, spatial light modulators, and optical switches.^{1,2} In general, these devices are based on a photo-optical effect, e.g., the photothermal/thermo-optic, the photorefractive, or the photochromic effect. In the first two cases, these effects can lead to self-focusing/defocusing in nonlinear optical materials, and enable diffraction-free or soliton-like propagation of optical light waves.^{3–5} Furthermore, the optically induced change of refractive index caused by a pump beam can be used to influence the propagation of a probe beam.⁶ This beam may have a different wavelength, and does not change the material's optical properties itself significantly.

For applications integrated optical devices may be preferred, as they enable high light intensities at moderate input power—in many cases, the speed of photo-optical effects scales about linearly with light intensity—and they are compatible with optical fibers. Recently we reported the self-focusing of an extraordinarily polarized guided beam in a planar waveguide in strontium–barium–niobate (SBN).⁷ Depending on the input power, a single collimated beam is strongly focused inside the sample up to diameters of several micrometers. For higher input power a splitting of the light in a sequence of several spots is observed.

The self-focusing originates from a positive refractive index change along the z axis, perpendicular to the propagation direction and the normal of the waveguiding layer. It can be explained qualitatively by thermal effects induced by light absorption: First, there is a direct thermo-optic effect, and second, a pyroelectric field can be generated that is screened by the large photoconductivity in the region of high light intensity.⁸ This screening can lead to a positive refractive

index change via the electro-optic effect, too. However, experimentally these two mechanisms cannot clearly be separated. Due to the small diameter of the light beam these effects are rather fast. The time constant for the buildup of the refractive index change is in the range well below 1 ms. In this letter we investigate the application of this effect for deflecting and switching of a probe beam of another wavelength that overlaps with the positive refractive index profile induced by the pump beam.

We use a congruently melting $\text{Sr}_{0.61}\text{Ba}_{0.39}\text{Nb}_2\text{O}_6$ crystal as a substrate with a doping of 0.2 wt % CeO_2 in the melt. The dimensions of the sample are $2 \times 5 \times 2.5 \text{ mm}^3$, where the 5 mm edges are along the c axis of the crystal. The propagation length is 2 mm. SBN shows large thermal effects. Both, the thermo-optic coefficient $\delta n_e / \delta T = 2.7 \times 10^{-4}$, and the change of the spontaneous polarization, $\delta P_s / \delta T = -8.5 \times 10^{-4} \text{ C K}^{-1} \text{ m}^{-2}$, are considerably large. Furthermore, the relatively small thermal conductivity $\lambda_t = 1.5 \text{ J K}^{-1} \text{ s}^{-1} \text{ m}^{-1}$ leads to large local temperature changes when the crystal is illuminated inhomogeneously. The cerium doping mainly increases light absorption in the green/blue wavelength region ($\alpha_e = 1.5 \text{ mm}^{-1}$ for $\lambda = 514.5 \text{ nm}$), whereas the absorption coefficient is low for red and infrared light ($\alpha_e = 0.17 \text{ mm}^{-1}$ for $\lambda = 632.8 \text{ nm}$).

Planar waveguides in oxide crystals can be fabricated by implantation of light ions with high energy into the polished top face of the crystal.⁹ In this work the SBN sample is irradiated at room temperature with He^+ ions at an energy of 2.0 MeV and a dose of $1 \times 10^{15} \text{ cm}^{-2}$. The implantation yields a buried damaged layer of decreased refractive index ($\Delta n_e \approx -0.02$ at $\lambda = 514.5 \text{ nm}$) at a depth of $4.5 \mu\text{m}$ that defines the waveguide thickness. Details of the fabrication and properties of these waveguides can be found in Ref. 10.

In the experimental setup, the beams of an argon ion laser ($\lambda = 514.5 \text{ nm}$) and/or a helium neon laser ($\lambda = 632.8$

^{a)}Electronic mail: dkip@physik.uni-osnabrueck.de

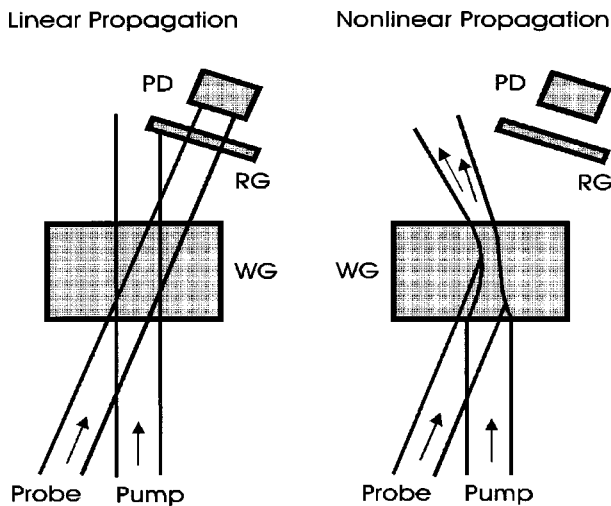


FIG. 1. Interaction scheme of pump (Ar^+ laser, dashed lines) and probe beam (HeNe laser, solid lines) inside the SBN waveguide (WG). The red beam is adjusted to intersect the green beam with a small linear shift and under a small angle. The arrows indicate the beam propagation direction. Behind the sample, the outcoupled light of the Ar^+ laser is blocked by a bandpass filter (RG). When the pump beam is off or when it has low intensity (linear propagation) the intensity of the red beam is measured by a photodiode (PD). When the pump beam is switched on (nonlinear propagation), the green beam is self-focused and self-bent to the left, trapping the red beam that moves away from the photodiode.

nm) are coupled into the SBN waveguide by microscope lenses [$40\times$ magnification ($\text{NA})=0.65$]. A cylindrical lens with a focal length of 250 mm is used at a distance of 270 mm to the first microscope lens to reduce the divergence of the light in the waveguide. An optical bandpass filter (Schott RG630) blocks the green light of the argon ion laser. The intensity distribution at the exit face of the sample is imaged on a charge coupled device (CCD) camera, and a photodiode with a small aperture allows power measurements at different positions of the outcoupled intensity spectrum.

The experiment is schematically illustrated in Fig. 1. When the power of the guided pump beam is too low to induce perceptible changes of the temperature distribution in the waveguiding layer, both the pump beam and the probe beam propagate in a linear regime ("linear propagation"). Their beam paths are nearly collimated in the waveguide, with beam radii ($1/e^2$ width) of about $50\ \mu\text{m}$ on the input face and about $35\ \mu\text{m}$ on the exit face of the sample. When the power of the pump beam increases, a change of the temperature is induced due to the increase of absorbed intensity in the region of the guided probe beam. This temperature change yields a positive change of the refractive index because of the thermo-optic effect and the screening of the pyroelectric field.⁸ The positive lens created in the waveguiding layer leads to self-focusing of the pump beam,⁷ and the red beam is trapped in the induced channel with increased refractive index, thus changing its original direction. When the green beam is self-focused to small diameters of a few micrometers, another mechanism becomes effective: the beam is also self-bent because of the photorefractive effect. As the red beam is already trapped by the pump beam, it follows the path of the green light which finally results in a significant deflection of the probe beam from its original position ("nonlinear propagation").

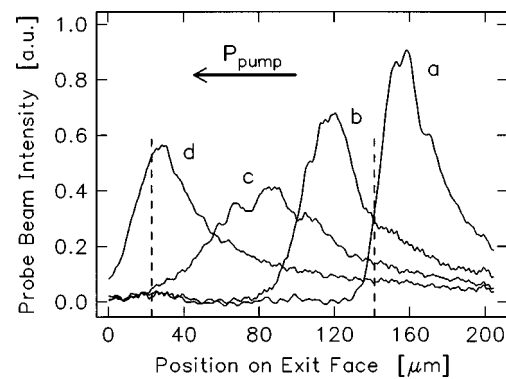


FIG. 2. Intensity distribution of the HeNe laser probe beam at the exit face of the planar SBN waveguide for different input pump power P_p of the Ar^+ laser. The intensity profiles are normalized to equal areas. The vertical dashed lines mark the approximate position of the green beam for low (right line) and for high ($P_p=19.7\ \text{mW}$, left line) pump power: (a) pump beam off; (b) $P_p=7.9\ \text{mW}$; (c) $P_p=13.3\ \text{mW}$; (d) $P_p=19.7\ \text{mW}$.

At first we investigate the beam deflection in our waveguide. In Fig. 2 the experimental steady state beam deflection of the red probe beam is shown as a function of the input power of the green pump beam. For zero or low input pump power, the probe beam propagates in the linear regime, i.e., no perceptible refractive index profile is induced by the pump beam. When the input pump power is increased, the probe beam is deflected. Moreover, in an intermediate regime of pump power, the probe beam is slightly broadened, and at high pump power it decreases again to nearly the initial diameter of $50\ \mu\text{m}$ for the case of low or zero input pump power, respectively.

The size of the deflection angle of the probe beam depends on the input power of the pump beam. In the measurement described above ($P_p < 20\ \text{mW}$), the deflection angle ranges from 20 to 70 mrad inside the sample. However, the largest beam deflection of the probe beam which we have obtained for an input power of the green pump beam of about 25 mW and an optimized adjustment of the intersection and spatial overlapping of probe and pump beam is 0.1 rad inside the sample. Including refraction at the exit face of the waveguide and the high refractive index of SBN, $n_e=2.284$, this gives a deflection angle of 0.23 rad for the outcoupled light in air.

For the investigation of all-optical switching of the probe beam we use a mechanical chopper in the path of the pump beam before it enters the waveguide. The maximum speed of the used chopper is restricted to frequencies below 3 kHz. A photodiode that measures the outcoupled light of the probe beam is adjusted to collect the light of the HeNe laser for the case where the pump light is off. When the pump beam is switched on, the probe beam is deflected and does not hit upon the photodiode anymore. A pump beam with a $1/e^2$ radius of $50\ \mu\text{m}$ and an input power of $P_p=25\ \text{mW}$ is used. This power is large enough to ensure a complete deflection of the probe beam for the steady state condition (when no chopper is used), and the remaining intensity of the probe beam reaching the photodiode in this case is well below 3% of the initial value.

The switching behavior of the probe beam for different frequencies of the modulated pump beam is presented in Fig. 3. The pulse form of the modulated pump beam is not ex-

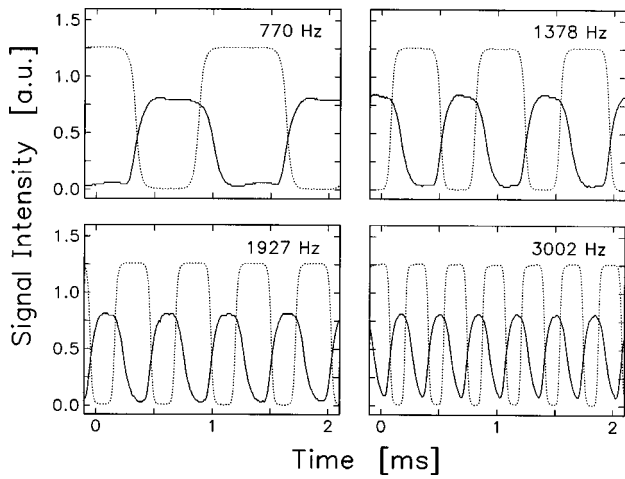


FIG. 3. Optical switching of the red probe beam (solid lines) for different frequencies of the mechanical chopper in the beam line of the green pump beam. For comparison the input pump power ($P_p=25$ mW) is shown by the dotted lines.

actually rectangular. This is due to the slit width of the chopper wheel that is only four to five times the beam diameter of the pump light. For low frequencies (e.g., 770 Hz) the pulse shape of the probe beam is similar to the form of the pump signal. With increasing frequency, the pulse shape of the probe beam becomes more sawtoothlike (e.g., 3 kHz). In this case the inverse chopper frequency comes close to the time constant for the buildup of the thermally induced refractive index distribution, and the plateau regions in the intensity signal of the probe beam observed for lower frequencies are not reached anymore. We use the peak-to-peak intensity of the probe beam as a figure of merit to describe the transmission bandwidth of this optical switch. The influence of changes in the pulse form of the probe signal is not included in this definition. The signal for the maximum chopper speed of 3 kHz decreases by less than 10% compared to the initial value at low frequency. Thus we can conclude that the bandwidth of the all-optical switch is still larger than that of the mechanical chopper used in the setup.

The buildup time for the refractive index changes is determined by thermal diffusion inside the sample. To estimate the *upper* time limit, we consider only the dimension z perpendicular to the propagation direction, i.e., heat diffusion along the z direction. Heat transport into the substrate and along the propagation direction are neglected within this approximation:

$$\frac{\delta T(z,t)}{\delta t} = \frac{\delta}{\delta z} \left(\frac{\lambda_t}{\rho c_p} \frac{\delta}{\delta z} T(z,t) \right) + \frac{\alpha_e}{\rho c_p} I(z,t). \quad (1)$$

Here $\rho=5.4 \times 10^3$ Kg m⁻³ is the specific density and $c_p=440$ J K⁻¹ kg⁻¹ the heat capacity of SBN. $T(z,t)$ and

$I(z,t)$ are the time dependent temperature and intensity distribution, respectively. The time constant $\tau_{th,max}$ for the buildup of the steady state temperature profile in the region of the guided light is proportional to the square of the beam radius w , and we get¹¹

$$\tau_{th,max} = \frac{\rho c_p w^2}{8 \lambda_t} \approx 0.5 \text{ ms} \quad (2)$$

for our experimental conditions. The real (experimental) time constant will be below this upper limit until we reduce the initial beam radius w strongly to values that are comparable with the waveguide thickness of 4.5 μ m. Following this approximation, smaller beam diameters of the pump beam should improve the speed of deflection and optical switching to a range larger than 10 kHz. Furthermore, an optimized design of the waveguide including heat sinks on the waveguide surface and/or substrate should enable a further improvement of the device.

In conclusion, strong thermally induced self-focusing, together with self-bending because of the photorefractive effect of a guided pump beam in a planar SBN waveguide, can be used for large angle deflection of a probe beam and for all-optical switching with time constants of fractions of milliseconds. Deflection angles of the outcoupled probe light up to 0.23 rad in air and frequencies up to 3 kHz for optical switching are reached in the experiment. Considerable improvements of the time constant for the buildup of the refractive index changes should be possible when the initial beam diameter of the pump light is decreased.

Financial support of the Deutsche Forschungsgemeinschaft (Project SFB 225, D9) is gratefully acknowledged.

- ¹H.M. Gibbs, *Optical Bistability: Controlling Light with Light* (Academic, Orlando, 1985).
- ²X. D. Cao, D. D. Meyerhofer, and G. P. Agrawal, *J. Opt. Soc. Am. B* **11**, 2224 (1994).
- ³M. Horowitz, R. Daisy, O. Werner, and B. Fischer, *Opt. Lett.* **17**, 475 (1992).
- ⁴G. Duree, J. L. Schultz, G. Salamo, M. Segev, A. Yariv, B. Crosignani, P. DiPorto, E. Sharp, and R. Neurgaonkar, *Phys. Rev. Lett.* **71**, 533 (1993).
- ⁵M. D. Iturbe-Castillo, P. A. Marquez-Aguilar, J. J. Sanchez-Mondragon, S. Stepanov, and V. Vysloukh, *Appl. Phys. Lett.* **64**, 408 (1994).
- ⁶E. D. Eugenieva, R. V. Roussev, and S. G. Dinev, *J. Mod. Opt.* **44**, 1127 (1997).
- ⁷D. Kip, E. Krätzig, V. Shandarov, and P. Moretti, *Opt. Lett.* **23**, 343 (1998).
- ⁸K. Buse, R. Pankrath, and E. Krätzig, *Opt. Lett.* **19**, 260 (1994).
- ⁹G. L. Destefanis, J. P. Gailliard, E. L. Ligeon, S. Valette, B. W. Farmery, P. D. Townsend, and A. Perez, *J. Appl. Phys.* **50**, 7898 (1979).
- ¹⁰D. Kip, B. Kemper, I. Nee, R. Pankrath, and P. Moretti, *Appl. Phys. B* **65**, 511 (1997).
- ¹¹H. J. Eichler, P. Günter, and D. W. Pohl, *Laser-Induced Dynamic Gratings* (Springer, Berlin, 1986).